

Drones for fluvial grain size measurement?

Journal:	<i>Earth Surface Processes and Landforms</i>
Manuscript ID	Draft
Wiley - Manuscript type:	Letters to ESEX
Date Submitted by the Author:	n/a
Complete List of Authors:	Woodget, Amy; University of Worcester, Institute of Science and Environment Austrums, Robbie; Independent Geospatial Consultant, Development
Keywords:	drone, river, grain size, structure from motion photogrammetry, gimbal

SCHOLARONE™
Manuscripts

Review

Drones for fluvial grain size measurement?

Amy S. Woodget¹ and Robbie Austrums²

¹Institute of Science and Environment, University of Worcester, Henwick Grove,
Worcester, WR2 6AJ, UK, ²Independent Geospatial Consultant, Richmond Road,
Worcester, UK

Abstract

Fluvial grain size plays a fundamental role in determining the condition and availability of aquatic habitats. Remote sensing provides rapid and objective methods of quantifying fluvial grain size, and typically provide coarse grain size outputs (c. 1m) at the catchment scale (up to 80km channel lengths) or fine resolution outputs (c. 1mm) at the patch scale (c. 1m²). Recently, drone based approaches have started to fill the gap between these scales, providing hyperspatial resolution data (<10cm) over reaches up to a few hundred metres in length. This 'mesoscale' is of importance to habitat assessments and is aligned with the ideals of the 'Riverscape' concept. Most drone based grain size measurement approaches use textural variables computed from drone orthoimagery. To date however, no published works provide quantitative evidence of the success of this approach, despite significant differences in platform stability and the image quality obtained by manned aircraft versus drones. With interest in drone surveys growing rapidly, such error quantification is essential for making reliable, evidence-based recommendations about the suitability of drones for routine management of fluvial environments. Here we provide an initial assessment of the accuracy and precision of grain size estimates produced using two different drone-based methods; (1) the

1 image textural variable 'negative entropy', and; (2) the roughness of point clouds
2 derived from drone imagery processed using structure from motion photogrammetry.
3 Data is collected from a small gravel-bed river in Cumbria, UK. Results from jack
4 knife analyses show that the point cloud roughness method gives more accurate and
5 precise measures of grain size at this site, as indicated by the mean (0.0002m) and
6 standard deviation (0.0184m) of residual errors. However, both methods struggle to
7 provide grain size measures with sub-centimetre precision. We suggest that blur
8 within the drone imagery prevents better precision, resulting from an inadequate
9 camera gimbal.

10

11 **Introduction**

12 The mapping and quantification of fluvial grain (or substrate) size is important in the
13 study of fluvial process, within both science and management. Grain size data are a
14 key input to hydraulic models, and are essential for quantifying sediment
15 entrainment, transfer and deposition. Our understanding of the interaction between
16 channel substrate and near-bed flow hydraulics relies on mapped grain size
17 distributions. Furthermore, the heterogeneity of bed material is an important
18 determinant of fluvial habitat availability, especially for spawning fish and benthic
19 macroinvertebrates (Wise and Molles, 1979; Keeley and Slaney, 1996; Evans and
20 Norris, 1997). The European Union's Water Framework Directive (European
21 Commission, 2000) recognises the importance of grain size in governing habitat
22 quality. Such data is required to help predict the ability of fluvial organisms to adapt
23 to extremes in flow level, which may result from regulated flow regimes, dam
24 constructions, hydro-peaking operations and changes in climate and weather
25 patterns (Goodwin et al., 2006; Habit et al., 2007; Garcia et al., 2011).

1
2
3 1
4
5 2 Traditional approaches to grain size mapping typically use visual classification
6
7 3 schemes such as the Wentworth Scale (Wentworth, 1922; Table 1). Users of this
8
9 4 classification include the UK's River Habitat Survey (Environment Agency 2003) and
10
11 5 the 'Physical Habitat Simulation System' (PHABSIM) devised by the United States
12
13 6 Fish and Wildlife Service but now used more widely (e.g. Centre for Ecology and
14
15 7 Hydrology, 2001). Quantitative methods usually involve in-situ or laboratory based
16
17 8 physical measurement of individual grains, including areal, grid, transect or
18
19 9 volumetric sampling (Wolman, 1954; Hey and Thorne, 1983; Church et al., 1987;
20
21 10 Rice and Church, 1996). Data collection of this type is never spatially continuous,
22
23 11 only sometimes spatially referenced, and rarely covers large spatial areas with great
24
25 12 detail. Furthermore, traditional approaches can be labour-intensive, time consuming
26
27 13 and often make assumptions about the representativeness of the spatially
28
29 14 discontinuous samples over larger areas (Leopold, 1970; Verdú et al., 2005). The
30
31 15 finer grain material is often under-sampled by a grid-by-number approach (Wolman,
32
33 16 1954; Church et al., 1987) and the removal of samples for volumetric analyses in the
34
35 17 laboratory can destroy the local patches of habitat that they are aiming to investigate
36
37 18 (e.g. freeze coring; Milan, 1996).
38
39
40
41
42
43
44

45 20 Since the 1970s, alternative methods of grain size quantification have made use of
46
47 21 remote sensing technologies, fuelled by the need for less subjective approaches,
48
49 22 which are non-invasive, reduce the time and effort spent in the field or laboratory and
50
51 23 provide more continuous spatial coverage at a range of scales (Table 2). Ongoing
52
53 24 advances in digital photogrammetry, digital image analysis and surveying
54
55 25 technologies mean that there is now an evolving body of remote sensing research
56
57
58
59
60

1 for grain size quantification, an overview of which is provided in Table 2. These
2 studies evidence the common trade-off between resolution (i.e. level of detail) and
3 coverage (i.e. extent of survey) which often afflicts remote sensing methods. No
4 single technique has yet proved its value for the rapid quantification of grain size at
5 the mesoscale; that is, with centimetric spatial resolution over channel lengths from
6 c. 50m to a few hundred metres. Yet such outputs would be of great value for
7 contributing to scientific understanding of mesohabitats and their applied
8 management (Frissell et al., 1986; Newson and Newson, 2000).

9
10 In recent years, dramatic development in the technology and applicability of drones
11 has provided an alternative approach for quantifying fluvial grain size. Drones are
12 sometimes known as 'unmanned aerial systems' (UAS), 'unmanned aerial vehicles'
13 (UAVs) or 'remotely piloted aircraft systems' (RPAS). Within this letter, we focus on
14 the use of small (< 7kg) drones which are often used in conjunction with novel
15 'structure from motion' digital photogrammetry (henceforth 'SfM') to derive fully
16 orthorectified and georeferenced aerial imagery and topographic data. Readers are
17 referred to Smith et al., (2015) and Eltner et al., (2016) for further detail on these
18 developments.

19
20 To date, very few published studies have applied drones and SfM for quantifying
21 fluvial grain size specifically. Those who have made progress in this area have
22 adapted the image texture methods of Carbonneau et al., (2004) used originally on
23 imagery acquired from manned aircraft. For instance, Tamminga et al., (2015)
24 acquired 5cm resolution imagery from a small, rotary-winged drone over a 1km
25 stretch of the Elbow River in Canada. Imagery was processed using digital

1
2
3 1 photogrammetry software EnsoMOSAIC (MosaicMill Ltd, Finland) to create an
4
5 2 orthophoto. Image texture, in the form of standard deviation of spectral values, was
6
7 3 computed from this imagery, using a 1m² moving window. Grain size calibration data
8
9 4 were acquired using close-range photo-sieving for 30 small sample plots (1m²),
10
11 5 where the B axes of 50 clasts were measured automatically using a Matlab routine.
12
13
14 6 The resulting relationship between image texture and grain size gave a strong
15
16 7 empirical correlation ($R^2 = 0.82$), which was subsequently used to estimate grain size
17
18 8 over the entire area of interest. Whilst the drone imagery itself was of hyperspatial
19
20 9 resolution (5cm), the nature of their approach means that Tamminga et al., (2015)
21
22 10 were only able to produce grain size predictions at a much coarser 1m spatial
23
24 11 resolution. Furthermore, they present no associated quantitative error assessment of
25
26 12 their predictions.
27
28
29
30
31

32 14 A similar approach was taken by de Haas et al., (2014) as part of a study exploring
33
34 15 the evolution of alluvial fan surfaces. Drone imagery was collected at a resolution of
35
36 16 4-6cm and processed using SfM and the texture approach of Carbonneau et al.,
37
38 17 (2012) to produce grain size outputs at 0.7m resolution of an area covering
39
40 18 0.745km². Relative motion blur was found to affect drone image quality, and was
41
42 19 attributed to a combination of cloudy conditions (which reduced light levels and
43
44 20 therefore necessitated increased exposure times) and wind gusts. Blurred parts of
45
46 21 the resulting orthophoto artificially reduced image texture outputs and adversely
47
48 22 affected the calibration with grain size. As a result, such areas were excluded from
49
50 23 the calibration. Validation of the model using independent grain size data is not
51
52 24 presented by de Haas et al., (2014) which again prohibits an understanding of the
53
54
55
56
57
58
59
60

1 accuracy of this texture approach and limits any real comparison against existing
2 techniques.

3
4
5
6
7
8
9
10 4 These papers highlight a need for robust and quantitative testing of grain size
11 estimations produced using drones and SfM. In addition, the development and
12 evaluation of alternative approaches which are less affected by spectral issues may
13 be of value. For example, 3D point cloud analysis methods developed for grain size
14 estimation using terrestrial laser scanner data (e.g. Heritage and Milan, 2009;
15 Brasington et al., 2012) may be applicable to drone imagery, as dense point clouds
16 are one of the outputs from SfM. Westoby et al., (2015) applied a drone and SfM
17 derived point cloud roughness approach to grain size quantification of an Antarctic
18 moraine, but were unable to obtain a strong calibration relationship ($R^2 = 0.225$)
19 between the standard deviation of elevation (i.e. roughness) and patch-scale D_{50}
20 measures (i.e. grain size). They report a mean grain size estimation error of -
21 2.90mm based on only five validation points, and do not report the precision of their
22 results. Woodget et al., (2016) provide an initial pilot study in a fluvial setting, where
23 point cloud roughness data were successfully used for grain size prediction ($R^2 =$
24 0.7712, mean error = -0.01mm, precision = 16.4mm). We build on these results
25 within this letter, using different and more comprehensive ground validation data.
26
27
28
29
30
31
32
33
34
35
36
37
38
39
40
41
42
43
44
45
46
47
48
49
50
51
52
53
54
55
56
57
58
59
60

25 **Site location**

1
2
3 1 We selected a c.120m long reach of Coledale Beck, a gravel-bed river located in
4
5 2 Cumbria for this research. The chosen reach comprises a meandering pool-riffle
6
7 3 system, with a bed composed predominantly of cobbles and boulders. The channel
8
9 4 features a number of large unvegetated point bars and opposing steep, undercut
10
11 5 banks. Variable grain sizes and a safe and accessible location for drone flying made
12
13 6 this a suitable site. Furthermore, the sediment dynamics of Coledale Beck are of
14
15 7 interest due to their downstream impacts on Bassenthwaite Lake. The lake is
16
17 8 designated as a National Nature Reserve and a Site of Special Scientific Interest,
18
19 9 partly due to its rare vendace (*Coregonus vandesius*) fish population. The spawning
20
21 10 grounds of this species are particularly sensitive to changes in the quantity and
22
23 11 quality of sediment within the lake. Increasing siltation of the lake is thought to be
24
25 12 partially responsible for the significant decline and subsequent extinction of the
26
27 13 vendace population (Orr and Brown, 2004). As a result, methods capable of mapping
28
29 14 and monitoring the evolution of sediment distribution within inflowing streams hold
30
31 15 potential for habitat evaluation and informing management strategies.
32
33
34
35
36
37
38

39 **Data acquisition and processing**

40 *Site set-up*

41
42
43 19 Prior to data collection at Coledale, we established four permanent markers at the
44
45 20 outer extents of the area of interest, using wooden stakes and circular survey
46
47 21 markers. All subsequent data collected using a Leica Builder 500 total station
48
49 22 (expected accuracy c. 1.5mm) were referenced to these markers using an arbitrary
50
51 23 local co-ordinate system.
52
53
54
55

56 *Drone survey*

1 We flew a Draganflyer X6 rotary-winged drone over the site at an altitude of c. 30m
2 above ground level. Flight control was entirely manual due to the lack of an autopilot
3 function. The drone was mounted with a small, consumer grade digital camera
4 (Panasonic Lumix DMC-LX3) held in a 1-axis brushless gimbal. The survey was
5 conducted in July 2013 during dry, bright and calm weather conditions. We
6 distributed 25 ground control points (GCPs) prior to the drone survey, ensuring they
7 were positioned to represent adequately the variation in topography across the site.
8 The GCPs were constructed from thin, black PVC sheeting, marked in a cross
9 pattern with white paint and, once positioned, were surveyed using the total station
10 relative to the local co-ordinate system (using the permanent markers). The relatively
11 short battery life on the drone (c. 6 minutes) meant that three flights were required to
12 cover the site with sufficient redundancy for subsequent processing using SfM. We
13 acquired a total of 88 images from the drone, of which we discarded 24 due to
14 blurring or unsuitable coverage.

16 *Structure from motion digital photogrammetry*

17 We imported the remaining 64 images into Agisoft's PhotoScan Professional digital
18 photogrammetry software, and processed them to create a c. 1cm resolution
19 orthophoto, a c. 2cm resolution digital elevation model (DEM), and dense 3D point
20 cloud, all referenced to the local co-ordinate system using the GCPs and permanent
21 markers. For further detail on the SfM process, readers are referred to Fonstad et al.,
22 (2013), Smith et al., (2015) and Eltner et al., (2016).

24 *Ground truth data*

1
2
3 1 For ground truthing purposes, we established 23 grain size sample plots along four
4 exposed bars at Coledale Beck (Figure 1). Each plot measured 40cm x 40cm. This
5
6 2
7 3
8 plot size was sufficiently large as to encompass the largest clasts within the field site,
9
10 4
11 but sufficiently small to ensure substrate size was as uniform as possible within the
12 5
13 plot itself. For each plot, a scaled, close-range photograph (e.g. Figure 1c) was
14 6
15 acquired using a handheld camera. These photographs were then georeferenced in
16 7
17 GIS to the site coordinate system, using a total station survey of each plot's four
18 8
19 corners. Within these plots, a sample of clasts were selected for measurement using
20 9
21 a 5cm x 5cm regular grid. Clasts falling beneath each grid node had their A- and B-
22 10
23 axis dimensions measured from the scaled photograph, unless they were deemed
24 11
25 unsuitable for measurement. Unsuitable clasts were those which were too small to
26 12
27 measure at a scale of 1:1, those which were largely obscured by other clasts, and
28 13
29 those which were not included fully within the photograph. Based on these data, we
30 14
31 computed grain size statistics for each plot, including the mean, D_{50} (grain size of the
32 15
33 50th percentile, or the median) and the D_{84} (grain size of the 84th percentile).
34
35
36
37
38
39

17 **Data analysis**

18 *Image texture*

19 We used the technique developed by Carbonneau et al., (2004) to compute image
20 texture from the orthophoto output. This empirical approach aims to establish a
21 statistical correlation between a given measure of image texture and grain size. We
22 computed image texture using a Matlab (Mathworks Inc.) routine on the red band of
23 the imagery (this is an arbitrary choice and the method would also work on other
24 bands). A square moving window with a kernel size of 41 pixels was passed over the
25 image at intervals of five pixels (the routine requires a kernel size of an uneven

1
2
3 1 number). A kernel size of 41 pixels is roughly equivalent to a kernel width of 41cm
4
5 2 and was selected based on *a priori* knowledge that maximum clast sizes at Coledale
6
7 3 Beck rarely exceed 40cm. We chose the interval size of five pixels as a compromise
8
9 4 between detail and processing time. As a result, texture outputs are produced at 5cm
10
11 5 resolution, but this could be altered as necessary. Within each kernel step, a
12
13 6 measure of image texture is calculated and assigned to the central pixel. Image
14
15 7 texture can be measured using a number of different metrics; in this case, we
16
17 8 calculated the 'negative image entropy'. This is a measure of image texture
18
19 9 calculated using a grey level co-occurrence matrix (GLCM), i.e. a grey-tone spatial
20
21 10 dependence probability distribution matrix first advocated by Haralick et al., (1973).
22
23 11 The matrix provides the probabilities of all pairwise (*i, j*) combinations of pixel grey
24
25 12 levels occurring within the specified moving window. The outputs are a function of
26
27 13 the angular relationship between a single pixel and its neighbours (*V*), and the
28
29 14 distance between them (the inter-pixel sampling distance, *D*). We chose to use
30
31 15 negative image entropy to compute image texture based on the work of Carbonneau
32
33 16 et al., (2004), however other measures are available and should be explored in
34
35 17 future. Negative image entropy provides a measure of randomness or the disorder of
36
37 18 pixel values and is calculated according to Equation 1;
38
39
40
41
42
43
44
45
46
47
48

$$\text{Negative Entropy} = \sum_{i,j} P_{i,j} (-\log P_{i,j})$$

49 *Equation 1*

50
51 *(after Haralick 1979)*
52
53
54
55

56 23 Where *P* is the co-occurrence matrix of the image within each step of the moving
57
58 24 window, based on the number of times that cells with grey levels *i* and *j* occur in two
59
60

1 pixels separated by set distance D and direction V , divided by the total number of
2 pixel pairs. The output is a map of negative image entropy, where higher values are
3 returned for more textured or heterogeneous parts of the image and lower values for
4 smoother or more homogeneous areas (Figure 2a). This image texture map was
5 then imported into GIS to permit statistical comparison with the ground-truthing
6 sample plots using linear regression.

8 *Point cloud roughness*

9 We exported the dense point cloud of the Coledale site from PhotoScan Pro (Agisoft
10 LLC) to the open source CloudCompare software (www.danielgm.net/cc/), and
11 assessed the need for detrending, filtering and smoothing of the cloud. Detrending
12 was found to be unnecessary but filtering and smoothing were required to reduce
13 noise within the cloud. This noise can introduce roughness to the point cloud which
14 does not result directly from grain size and therefore must be removed. A filtering
15 and smoothing procedure was written in-house. We filtered the cloud by taking the
16 mean of the interquartile range in elevation within 6mm x 6mm cells and smoothed
17 the cloud by averaging elevation values within a 2.5cm radius moving window. We
18 performed a visual sensitivity check on the filtering cell size and smoothing window
19 size, to ensure that sufficient noise was removed whilst preserving as much of the
20 topographic detail within the cloud as possible.

21
22 Next we used CloudCompare's inbuilt roughness tool to compute roughness values
23 for each point in the smoothed and filtered cloud. Roughness is defined as the
24 distance between each point in the cloud and the least squares best fitting plane
25 computed on its nearest neighbours within a spherical kernel of a specified size.

1
2
3 1 Roughness was computed for a kernel radius size of 20cm, again based on *a priori*
4
5 2 knowledge of typical grain sizes at Coledale Beck. Lastly, we rasterised roughness
6
7 3 outputs at 3cm resolution (Figure 2b), exported them to ArcGIS and computed
8
9 4 roughness statistics on a plot by plot basis for subsequent linear regression against
10
11 5 the ground truth data.
12
13
14 6

15 7 *Jack knife analysis*

16
17 8 Linear regressions of image texture and roughness with grain size for each of our
18
19 9 sample plots provide calibration relationships for predicting grain size over the wider
20
21 10 area of interest. Validation is also required to assess the accuracy and precision of
22
23 11 grain size estimates. We validated our calibration relationships using a jack knife
24
25 12 approach (Quenouille 1949, Tukey 1958), an iterative method which excludes one
26
27 13 ground truth plot at a time, and uses the linear regression equation based on the
28
29 14 remaining plots to predict grain size for the excluded plot. We compared the
30
31 15 measured grain size for each plot to the equivalent predicted grain size, to assess
32
33 16 the strength of the predictive relationship. Measured grain sizes were also subtracted
34
35 17 from the predicted grain sizes on a plot by plot basis to obtain residual error values.
36
37 18 The average and standard deviation of the residuals for all plots are taken to
38
39 19 represent the overall accuracy and precision of grain size estimates.
40
41
42
43
44
45
46
47
48
49
50
51
52
53
54
55
56
57
58
59
60

21 **Results**

22 22 Calibration and validation relationships for grain size predictions using image texture
23
24 23 and roughness approaches are presented in Table 3 and Figures 3-4. We found that
25
26 24 maximum negative entropy and average roughness values correlated against D_{84} of
27
28 25 the B axes produced the strongest calibration relationships (Table 3). Our results

1 demonstrate that for this site, the point cloud roughness approach to grain size
2 estimation gives both stronger calibration and validation relationships, as indicated
3 by the slope and R^2 values. Furthermore, grain sizes predicted using the roughness
4 method are almost two orders of magnitude more accurate than those predicted
5 using the image texture method, as indicated by the mean of residual errors.
6 Precision, represented by the standard deviation of residual errors, is greater than
7 1cm for both approaches.

8

9 **Discussion**

10 Within this paper we have, for the first time, quantified the accuracy and reliability of
11 an image texture and a point cloud roughness approach to grain size quantification
12 using drone imagery and digital photogrammetry. The high resolution, quantitative,
13 objective, spatially continuous, spatially explicit results are easily computed and have
14 potential to aid our understanding of sediment dynamics and habitat heterogeneity at
15 the mesoscale within a riverscape style framework (Fausch et al., 2002). However,
16 our results raise three important and interlinked questions;

17

18 *(1) Why does our image texture approach not produce calibration relationships of*
19 *similar strength to those reported by others (de Haas et al., 2014, Tamminga et al.,*
20 *2015)?*

21

22 Weak calibration and validation relationships between image texture and grain size,
23 and poor residual errors, will occur when image texture is influenced by factors other
24 than grain size. These factors might include the use of blurred imagery, the effects of
25 local topographic shadowing, the presence of vegetation or water, and notable

1 variations in grain colour (i.e. lithology). Relative motion blur, a consequence of (a)
2 increased exposure times resulting from cloudy conditions and (b) wind gusts, are
3 noted by de Haas et al., (2014) as a significant problem in predicting grain sizes
4 using image texture. They note that quantitative correction of relative motion blur
5 could not be conducted because their fixed-wing drone was not equipped with the
6 accelerometers necessary to provide correction data. The specification of the gimbal
7 used is not presented by de Haas et al., (2014), however, given the age of the drone
8 model they use, we anticipate a gimbal which is rather more rudimentary than the 3-
9 axis stabilisation mounts often available today. As a result, the approach of de Haas
10 et al., (2014) is to side-step the issue by excluding any blurred sections of the
11 orthophoto from further analysis, to achieve strong calibrations with grain size ($R^2 =$
12 0.82). However, such manual interventions can be time consuming and may result in
13 inadequate site coverage or necessitate extra field time. Furthermore, the issue of
14 image blurring remains unaddressed. Tamminga et al., (2015) find that shadows also
15 disrupt calibration relationships by introducing high texture values in areas of
16 pronounced topographic relief and vegetation, which in turn result in erroneously
17 high grain size predictions. However, the 3-axis stabilised gimbal used on their
18 Aeryon Scout drone helps to reduce image blur, permitting another strong calibration
19 with grain size ($R^2 = 0.82$). In this paper, we use a basic 1-axis camera gimbal on our
20 drone, which was flown in calm wind conditions. Whilst efforts were made to remove
21 blurred images before photogrammetric processing, areas of blurring are evident on
22 the resulting orthophoto which is then used to develop the empirical calibration with
23 grain size. Alongside the minor influence of vegetation presence and minor
24 variations in grain colour within some of the ground truth plots, we expect that this
25 gimbal is the main reason for the poorer calibration with grain size than reported

1
2
3 1 elsewhere. However, further dedicated testing is required to prove this, and
4
5 2 subsequently to reduce the incidence of blurring or improve our ability to detect and
6
7 3 eliminate it from images. Some initial work on blur detection and removal is provided
8
9
10 4 by Sieberth et al., 2013 and Sieberth et al., 2016. Future work might also explore the
11
12 5 use of texture metrics other than negative entropy for improving a calibration with
13
14 6 grain size.

15
16
17
18 8 *(2) Why does our point cloud roughness approach perform so much better than our*
19
20 9 *image texture approach (Table 3)?*

21
22
23
24
25 11 Our point cloud roughness method was conceived out of a need to move away from
26
27 12 the adverse effects of blurred drone imagery. Given that exactly the same drone
28
29 13 imagery is used as input for both texture and roughness approaches though, we
30
31 14 might expect the roughness approach to be adversely affected by blur too. The SfM-
32
33 15 photogrammetry process computes indirect measures of elevations using drone
34
35 16 image parallax, to create a point cloud. Thus where image quality is poor (e.g. due to
36
37 17 blurring) or lacking in texture (e.g. spectrally homogeneous areas) then greater
38
39 18 amounts of noise (i.e. erroneous point matches) are likely to be observed. More
40
41 19 generally, we would expect other factors to influence the point cloud roughness-grain
42
43 20 size relationship, including;

- 44
45
46
47 21 • Presence of vegetation – where topographic variation in the point cloud is not
48
49 22 a result of variation in grain size.
- 50
51
52 23 • Interstitial spaces between large clasts which are occupied by smaller clasts -
53
54 24 where topographic variation is high within the extent of the kernel but grain
55
56 25 size is low.

- Complex levels of topographic variation over short distances – where features such as footprints introduce variation which does not result from grain size and cannot be removed easily by detrending.
- Packing and imbrication of clasts – where partially buried clasts do not produce the same topographic signature as exposed clasts of equivalent size, a well-known issue for a number of grain size quantification methods (e.g. Church et al., 1987; Sime and Ferguson, 2003; Heritage and Milan, 2009; Picco et al., 2013).

Despite these complicating factors, we are still able to predict grain sizes with exceptionally low mean residual errors (<1mm). We suggest that it is only by implementing the smoothing and filtering procedures described earlier that this has been possible. We also note that the standard deviation of residual errors is much higher (>1cm), indicating a lack of precision and reliability of our roughness grain size predictions, which probably results from point cloud noise. As a result, further systematic research is required to improve precision, regardless of such low mean errors.

(3) Which remote sensing approach is “best” for quantifying fluvial grain size?

The accuracy and precision of our results for a point cloud roughness method indicates that they are roughly in line with or better than other remote sensing approaches for grain size quantification (Table 2), including other drone based approaches (e.g. Westoby et al., 2015). The spatial resolution of our outputs is also finer than those approaches with similar mean accuracy levels (Table 2). However, we note that the slope of the observed versus predicted relationship for point cloud roughness (0.7752, Figure 4) is lower than those reported by Carbonneau et al.,

1 (2004) and Carbonneau et al., (2005b) for the use of an image texture approach of
2 imagery acquired from a manned aircraft (Table 2). Again, we anticipate platform
3 stability and image clarity to be responsible for this difference. Ultimately, the choice
4 of the “best” method for quantifying fluvial substrate size will be determined by the
5 specific requirements of a given application, including the required scale, spatial
6 coverage, accuracy, precision, data acquisition and processing times and costs. At
7 present, our point cloud roughness approach is best suited to studies requiring
8 coverage of up to c. 1km channel length with spatial resolutions of a few centimetres.
9 However, with rapid and on-going developments in drone, gimbal, sensor and
10 software technology as well as associated processing algorithms, we anticipate that
11 covering larger areas with greater detail and at lower costs will only become more
12 practicable with time.

13 14 *Future work*

15 Future research should aim to reduce the impact of image blur on both image texture
16 and point cloud roughness approaches. For example, we intend to compare the
17 results obtained using different camera gimbals and conduct sensitivity analysis to
18 determine the most appropriate kernel sizes for calculating image texture and point
19 cloud roughness. Further consideration of scale and quantification of the range of
20 grain sizes which can be predicted accurately and reliably is also of importance. For
21 instance, the use of the 2.5cm radius smoothing kernel means that reliable prediction
22 of grain sizes smaller than 5cm is compromised at present. A reduction of image blur
23 should reduce point cloud noise and thereby permit a smaller smoothing kernel size
24 to be used and enable prediction of smaller grain sizes. Such enhanced research is
25 necessary to help us fully understand the potential for upscaling and transferability of

1
2
3 1 this method to different fluvial settings and other environments, including submerged
4
5 2 areas.

3 **Conclusion**

4 Within this letter we have provided an initial quantitative assessment of two
5 approaches to fluvial grain size measurement using drone imagery processed with
6 SfM digital photogrammetry. We flew a rotary-winged drone over a gravel bed river
7 in the English Lake District and processed the resultant imagery into an orthophoto,
8 DEM and point cloud. An empirical relationship was developed between validation
9 grain size data and grain sizes predicted using (a) an image texture approach on the
10 orthophotos and (b) a roughness approach on the point cloud. Our error assessment
11 reveals poor calibration and validation results for the texture approach, as well as
12 poor accuracy and precision of grain size estimates. We suspect this is due to
13 blurred imagery caused by an inadequate camera gimbal. Point cloud roughness is
14 much better correlated with grain size and produces much lower mean errors. Whilst
15 smoothing and filtering of the point cloud has permitted very accurate grain size
16 estimations on a plot by plot basis, precision is weaker, highlighting the need for
17 improvements to the reliability of this roughness method. The use of either technique
18 requires careful consideration of potential error sources and, crucially, the effects of
19 any degradation in image clarity. With further work, these methods have potential to
20 be of value to a range of river habitat research and management applications. Direct
21 measurements of surface roughness using the point cloud may also provide input to
22 applications beyond habitat assessment, including studies of flow resistance and
23 hydraulic modelling.

24 25 **Acknowledgments**

1
2
3 1 We are very grateful to Patrice Carbonneau for the image texture processing, to
4
5 2 Fleur Visser, Richard Johnson, James Atkins, Andy Skellern, Jeff Warburton, Carl
6
7 3 Greenman and Milo Creasey for field assistance, and to the landowners for
8
9 4 permitting us access to the site. This research was funded by the University of
10
11 5 Worcester (PhD studentship for Amy Woodget) and a student research award from
12
13 6 the Geological Remote Sensing Group, a special interest group of The Geological
14
15 7 Society of London and the Remote Sensing and Photogrammetry Society.
16
17
18
19
20
21
22

23 **References**

- 24
25 11 Adams, J. 1979. Gravel size analysis from photographs. *Journal of the Hydraulics*
26 12 *Division, Proceedings of the American Society of Civil Engineers*, 105, HY10: 1247-
27 13 1255
28
29 14
30 15 Brasington, J., Vericat, D. and Rychov, I. 2012. Modeling river bed morphology,
31 16 roughness, and surface sedimentology using high resolution terrestrial laser
32 17 scanning. *Water Resources Research* 48 W11519, doi: 10.1029/2012WR012223
33 18
34 19 Buscombe, D. 2008. Estimation of grain size distributions and associated
35 20 parameters from digital images of sediment. *Sedimentary Geology* 210: 1-10
36 21
37 22 Buscombe, D. 2013. Transferable wavelet method for grain-size distribution from
38 23 images of sediment surface and thin section, and other natural granular patterns.
39 24 *Sedimentology* 60 (7): 1709-1732.
40 25
41 26 Buscombe, D. and Masselink, G. 2009. Grain-size information from the statistical
42 27 properties of digital images of sediment. *Sedimentology* 56: 421-438
43 28
44 29 Buscombe, D. Rubin, D.M. and Warrick, J.A. 2010. A universal approximation of
45 30 grain size from images of noncohesive sediment. *Journal of Geophysical Research*
46 31 115 F02014 doi: 10.1029/2009JF001477
47 32
48 33 Butler, J.B., Lane, S.N, and Chandler, J.H. 2001. Automated extraction of grain-size
49 34 data from gravel surfaces using digital image processing. *Journal of Hydraulic*
50 35 *Research* 39 (4): 519-529
51 36
52
53
54
55
56
57
58
59
60

- 1
2
3 1 Carbonneau, P.E., Lane, S.N. and Bergeron, N. 2004. Catchment-scale mapping of
4 2 surface grain size in gravel bed rivers using airborne digital imagery. *Water*
5 3 *Resources Research* 40, W07202, doi:10.1029/2003WR002759
6 4
7 4
8 5 Carbonneau, P.E., Bergeron, N.E. and Lane, S.N. 2005a. Texture-based
9 6 segmentation applied to the quantification of superficial sand in salmonids river
10 7 gravels. *Earth Surface Processes and Landforms* 30: 121-127
11 8
12 8
13 9 Carbonneau, P.E., Bergeron, N. and Lane, S.N. 2005b. Automated grain size
14 10 measurements from airborne remote sensing for long profile measurements of fluvial
15 11 grain sizes. *Water Resources Research* 41, W11426, doi:10.1029/2005WR003994
16 12
17 12
18 13 Carbonneau, P.E., Fonstad, M.A., Marcus, W.A., and Dugdale, S.J. 2012. Making
19 14 riverscapes real. *Geomorphology* 137 (1): 74-86
20 15
21 15
22 16 Centre for Ecology and Hydrology. 2001. Further validation of PHABSIM for the
23 17 habitat requirements of salmonid fish. Final project report to Environment Agency
24 18 (W6-036) and CEH (C00962)
25 19
26 19
27 20 Church, M.A. McLean, D.G. and Wolcott, J.F. 1987. River bed gravels: Sampling and
28 21 Analysis, In Thorne, C.R., Bathurst, J.C. and Hey, R.D. (Eds) *Sediment Transport in*
29 22 *Gravel-bed Rivers*, John Wiley and Sons, Chichester
30 23
31 23
32 24 De Haas, T., Ventra, D., Carbonneau. P. and Kleinhan, M.G. 2014. Debris flow
33 25 dominance of alluvial fans masked by runoff reworking and weathering.
34 26 *Geomorphology* 217: 165-181
35 27
36 27
37 28 Eltner, A., Kaiser, A., Castillo, C., Rock, G., Neugirg, F. and Abellán, A. 2016. Image-
38 29 based reconstruction in geomorphometry – merits, limits and developments. *Earth*
39 30 *Surface Dynamics* 4: 359-389
40 31
41 31
42 32 Entwistle, N.S. and Fuller, I.C. 2009. Terrestrial laser scanning to derive the surface
43 33 grain size facies character of gravel bars. In Heritage, G.L. and Large, A.R.G. (Eds)
44 34 *Laser Scanning for the Environmental Sciences*, Wiley-Blackwell, London
45 35
46 35
47 36 European Commission. 2000. Directive 2000/60/EC of the European Parliament and
48 37 of the Council of 23rd October 2000: Establishing a framework for Community action
49 38 in the field of water policy. *Official Journal of the European Communities*, Brussels,
50 39 22.12.2000, L327: 1-72
51 40
52 40
53 40
54 41 Evans, L.J. and Norris, R.H. 1997. Prediction of benthic macroinvertebrate
55 42 composition using microhabitat characteristics derived from stereo photography.
56 43 *Freshwater Biology* 37: 621-633
57 44
58 44
59
60

- 1
2
3 1 Fausch, K.D., Torgersen, C.E., Baxter, C.V. and Hiram, L.W. 2002. Landscapes to
4 2 riverscapes: bridging the gap between research and conservation of stream fishes.
5 3 BioScience 52 (6): 483-498
6 4
7 5 Fonstad, M.A., Dietrich, J.T., Courville, B.C., Jensen, J.L. and Carbonneau, P.E.
8 6 2013. Topographic structure from motion: a new development in photogrammetric
9 7 measurement. Earth Surface Processes and Landforms 38 (4): 421-430
10 8
11 9 Frissell, C.A., Liss, W.J., Warren, C.E. and Hurley, M.D. 1986. A hierarchical
12 10 framework for stream habitat classification: viewing streams in a watershed context.
13 11 Environmental Management 10 (2): 199-214
14 12
15 13 Garcia, A., Jorde, K., Habit, E., Caamano, D. and Parra, O. 2011. Downstream
16 14 environmental effects of dam operations: changes in habitat quality for native fish
17 15 species. River Research and Applications 27: 312-327
18 16
19 17 Goodwin, P., Jorde, K., Meier, C. and Parra, O. 2006. Minimizing environmental
20 18 impacts of hydropower development: transferring lessons from past projects to a
21 19 proposed strategy for Chile. Journal of Hydroinformatics 8: 253-270
22 20
23 21 Graham, D.J., Reid, I. and Rice, S.P. 2005a. Automated sizing of coarse-grained
24 22 sediments: image- processing procedures. Mathematical Geology 37(1): 1-28
25 23
26 24 Graham, D.J., Rice, S.P. and Reid, I. 2005b. A transferable method for the
27 25 automated grain sizing of river gravels. Water Resources Research 41, W07020,
28 26 doi:10.1029/2004WR003868
29 27
30 28 Habit, E., Belk, M.C. and Parra, O. 2007. Response of the riverine fish community to
31 29 the construction and operation of a diversion hydropower plant in central Chile.
32 30 Aquatic Conservation: Marine and Freshwater Ecosystems 17: 37-49
33 31
34 32 Haralick, R.M., Shanmugam, K. and Dinstein, I. 1973. Textural features for image
35 33 classification. IEEE Transactions on Systems, Man and Cybernetics SMC-3 (6): 610-
36 34 621
37 35
38 36 Haralick, R.M. 1979. Statistical and structural approaches to texture. Proceedings of
39 37 the IEEE 67 (5): 786-804
40 38
41 39 Heritage, G.L. and Milan, D.J. 2009. Terrestrial laser scanning of grain roughness in
42 40 a gravel-bed river. Geomorphology 113: 4-11
43 41
44 42 Hey, R.D. and Thorne, C.R. 1983. Accuracy of surface samples from gravel bed
45 43 materials. Journal of Hydraulic Engineering 109 (6): 842-851
46 44
47
48
49
50
51
52
53
54
55
56
57
58
59
60

- 1
2
3 1 Hodge, R., Brasington, J. and Richards, K. 2009. In situ characterization of grain-
4 2 scale fluvial morphology using Terrestrial Laser Scanning. *Earth Surface Processes*
5 3 and *Landforms* 34: 954-968
6 4
7 4
8 5 Ibbeken, H. and Schleyer, R. 1986. Photo-sieving: a method for grain size analysis
9 6 of coarse-grained, unconsolidated bedding surfaces. *Earth Surface Processes* and
10 7 *Landforms* 11: 59-77
11 8
12 8
13 9 Keeley, E.R. and Slaney, P.A. 1996. Quantitative measures of rearing and spawning
14 10 habitat characteristics for stream-dwelling salmonids: guidelines for habitat
15 11 restoration. Province of British Columbia, Ministry of Environment, Lands and Parks,
16 12 and Ministry of Forests. *Watershed Restoration Project Report 4*
17 13
18 13
19 14 Leopold, L.B. 1970. An improved method for size distribution of stream bed gravel.
20 15 *Water Resources Research* 6 (5): 1357-1366
21 16
22 16
23 17 Milan, D.J. 1996. The application of freeze-coring for siltation assessment in a
24 18 recently regulated stream. *Hydrologie dans les pays celtiques*, Rennes, France 8-11
25 19 July 1996. Ed. INRA Paris (Les Colloques 79)
26 20
27 20
28 21 Milan, D.J. and Heritage, G.L. 2012. LiDAR and ADCP use in gravel-bed rivers:
29 22 Advances since GBR6. In Church, M., Biron, P. and Roy, A. (Eds) *Gravel-bed*
30 23 *Rivers: Processes, Tools, Environments*, Wiley-Blackwell, Chichester
31 24
32 24
33 25 Newson, M.D. and Newson, C.L. 2000. Geomorphology, ecology and river channel
34 26 habitat: mesoscale approaches to basin-scale challenges. *Progress in Physical*
35 27 *Geography* 24 (2): 195-217
36 28
37 28
38 29 Orr, H. and Brown, D. 2004. Bassenthwaite Lake Geomorphological Study Findings:
39 30 Summary Report, Environment Agency Publication Reference ScNW0904BIGO-E-P
40 31
41 31
42 32 Picco, L., Mao, L., Cavalli, M., Buzzi, E., Rainato, R. and Lenzi, M.A. 2013.
43 33 Evaluating short-term morphological changes in a gravel-bed braided river using
44 34 terrestrial laser scanner. *Geomorphology* 201: 323-334
45 35
46 35
47 36 Quenouille, M.H. 1949. Approximate tests of correlation in time-series. *Journal of the*
48 37 *Royal Statistical Society Series B* 11: 68-84
49 38
50 38
51 39 Rice, S. and Church, M. 1996. Sampling surficial fluvial gravels: the precision of size
52 40 distribution percentiles estimates. *Journal of Sedimentary Research* 66 (3): 654-665
53 41
54 41
55 42 Rubin, D.M. 2004. A simple autocorrelation algorithm for determining grain size from
56 43 digital images of sediment. *Journal of Sedimentary Research* 74 (1): 160-165
57 44
58 44
59
60

- 1
2
3 1 Rychov, I., Brasington, J. and Vericat, D. 2012. Computational and methodological
4 2 aspects of terrestrial surface analysis based on point clouds. *Computers and*
5 3 *Geosciences* 42: 64-70
6 4
7 5 Sieberth, T., Wackrow, R. and Chandler, J.H. 2013. Automation isolation of blurred
8 6 images from UAV image sequences. *International Archives of Photogrammetry,*
9 7 *Remote Sensing and Spatial Information Sciences*, XL-1/W2: 361-366
10 8
11 9 Sieberth, T., Wackrow, R. and Chandler, J.H. 2016. Automatic detection of blurred
12 10 images in UAV image sets. *ISPRS Journal of Photogrammetry and Remote Sensing*
13 11 122: 1-16
14 12
15 13 Sime, L. C. and Ferguson, R. I. 2003. Information on grain sizes in gravel-bed rivers
16 14 by automated image analysis. *Journal of Sedimentary Research* 73 (4): 630-636
17 15
18 16 Smith, M.W., Carrick, J.L. and Quincey, D.J. 2015. Structure from motion
19 17 photogrammetry in physical geography. *Progress in Physical Geography* 40 (2): 247-
20 18 275
21 19
22 20 Tamminga, A., Hugenholtz, C., Eaton, B. and LaPointe, M. 2015. Hyperspatial
23 21 remote sensing of channel reach morphology and hydraulic fish habitat using an
24 22 unmanned aerial vehicle (UAV): A first assessment in the context of river research
25 23 and management. *River Research and Applications* 31 (3): 379-391
26 24
27 25 Tukey, J.W. 1958. Bias and confidence in not-quite large samples. *Annals of*
28 26 *Mathematical Statistics* 29: 614
29 27
30 28 Verdú, J.M., Batalla, R.J. and Martinez-Casasnovas, J.A. 2005. High-resolution
31 29 grain-size characterisation of gravel bars using imagery analysis and geo-statistics.
32 30 *Geomorphology* 72: 73-93
33 31
34 32 Wentworth, C.K. 1922. A scale of grade and class terms for clastic sediments.
35 33 *Journal of Geology* 30: 377-392
36 34
37 35 Westoby, M.J., Dunning, S.A., Woodward, J., Hein, A.S., Marrero, S.M., Winter, K.
38 36 and Sugden, D.E. 2015. Sedimentological characterization of Antarctic moraines
39 37 using UAVs and Structure-from-Motion photogrammetry. *Journal of Glaciology* 61
40 38 (230): 1088-1102
41 39
42 40 Wise, D.H. and Molles, M.C. 1979. Colonisation of artificial substrate by stream
43 41 insects: influence of substrate size and diversity. *Hydrobiologia* 65 (1): 69-74
44 42
45 43 Wolman, M.G. 1954. A method of sampling coarse river-bed material. *Transactions*
46 44 *of the American Geophysical Union* 35 (6): 951-956
47
48
49
50
51
52
53
54
55
56
57
58
59
60

Woodget, A.S., Visser, F., Maddock, I.P. and Carbonneau, P. 2016. Quantifying fluvial substrate size using hyperspatial resolution UAS imagery and SfM-photogrammetry. Extended Abstract, 11th International Symposium on Ecohydraulics, Melbourne, Australia, 7-12 February

Table 1. The Wentworth Scale of particle size definitions (after Wentworth, 1922).

Size range		Wentworth Class
Phi (ϕ)	Metric (mm)	
<-8	>256	Boulder
-6 to -8	64-256	Cobble
-5 to -6	32-64	Very coarse gravel
-4 to -5	16-32	Coarse gravel
-3 to -4	8-16	Medium gravel
-2 to -3	4-8	Fine gravel
-1 to -2	2-4	Very fine gravel
0 to -1	1-2	Very coarse sand
1 to 0	0.5-1	Coarse sand
2 to 1	0.25-0.5	Medium sand
3 to 2	0.125-0.25	Fine sand
4 to 3	0.0625-0.125	Very fine sand
8 to 4	0.0039-0.0625	Silt
>8	<0.0039	Clay

Table 2. An overview of remote sensing methods for quantifying fluvial grain sizes.

Method	Theory	Extent	Typical Resolution	Typical Accuracy	Typical Precision	Slope (Obs v. Pred)	Limitations	References
Close-range photo-sieving	Manual or automated analyses of photos acquired from tripod-mounted cameras to measure individual grains	Patch level (microscale)	< 1cm	<0.25 phi	?	?	Under- and over-estimations of grain sizes reported by different papers	Adams, 1979; Ibbeken and Schleyer, 1986; Butler et al., 2001; Sime and Ferguson, 2003; Graham et al., 2005a; Graham et al., 2005b
Statistical image analysis	Decomposition of the 2D spectral signatures of images to quantify grain sizes	Patch level (microscale)	<1mm	<3mm	?	?	Extensive site-specific look-up data typically required	Rubin, 2004; Buscombe, 2008; Buscombe and Masselink, 2009; Buscombe et al., 2010; Buscombe 2013
Image textural analysis	Computed image textural variables are correlated with field measures from small patches	Reach to catchment level	c. 1m	3-8mm	13.9-29mm	1.03-1.23	Labour intensive and time consuming collection of field data required for calibration purposes	Carbonneau et al., 2004; Carbonneau et al., 2005a; Carbonneau et al., 2005b; Verdú et al., 2005
Terrestrial laser	Variations of roughness	Patch (microscale)	c. 5cm	c. 1mm	2.34cm	0.5261	Requires significant field	Entwistle and Fuller, 2009;

1
2
3
4
5
6
7
8
9
10
11
12
13
14
15
16
17
18
19
20
21
22
23
24
25
26
27
28
29
30
31
32
33
34
35
36
37
38
39
40
41
42
43
44
45
46
47
48
49

scanning	(standard deviation) in laser-derived point clouds to estimate grain sizes	e) to reach level					and processing efforts to cover large areas (including de-trending)	Heritage and Milan, 2009; Hodge et al., 2009; Brasington et al., 2012; Milan and Heritage, 2012; Rychov et al., 2012
----------	--	-------------------	--	--	--	--	---	--

For Peer Review

1
2
3
4
5
6
7
8
9
10
11
12
13
14
15
16
17
18
19
20
21
22
23
24
25
26
27
28
29
30
31
32
33
34
35
36
37
38
39
40
41
42
43
44
45
46
47
48
49

Table 3. Comparison of calibration, validation and residual errors between the image texture and point cloud roughness approaches to grain size quantification.

		Image texture	Point cloud roughness
Calibration	R ²	0.2987	0.7983
	Slope	0.0006	12.347
	Intercept	-0.3479	-0.0028
Validation	R ²	0.1601	0.7551
	Slope	0.2051	0.7752
	Intercept	0.0605	0.0121
Residual errors	Mean (m)	0.0186	0.0002
	Standard deviation (m)	0.0343	0.0184

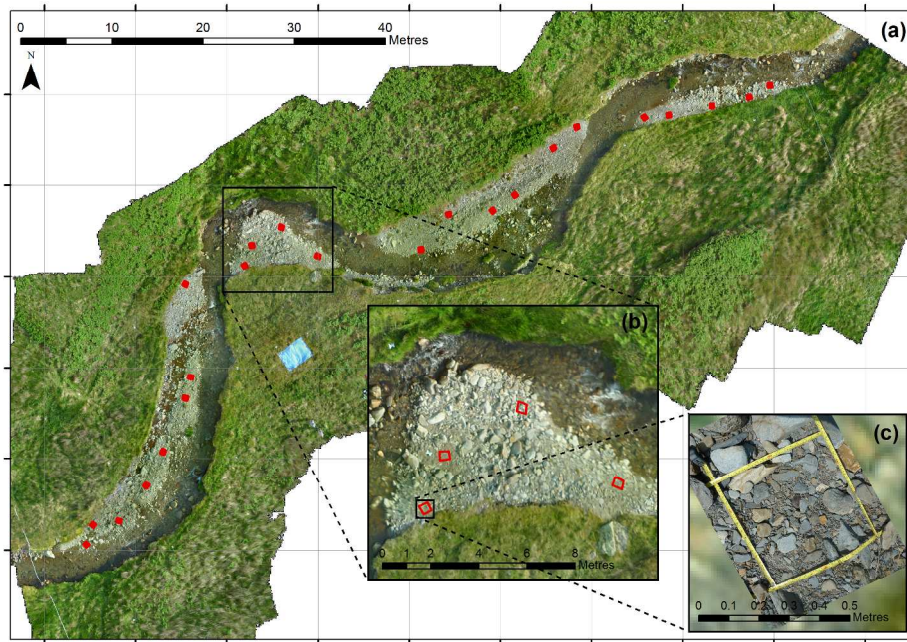


Figure 1. (a) Location of the ground truth validation plots at Coledale Beck, shown over the orthophotos, with close-up views shown in inset maps (b) and (c). Close-range georeferenced photo example for one of the ground truth sample plots is given in (c).

296x210mm (300 x 300 DPI)

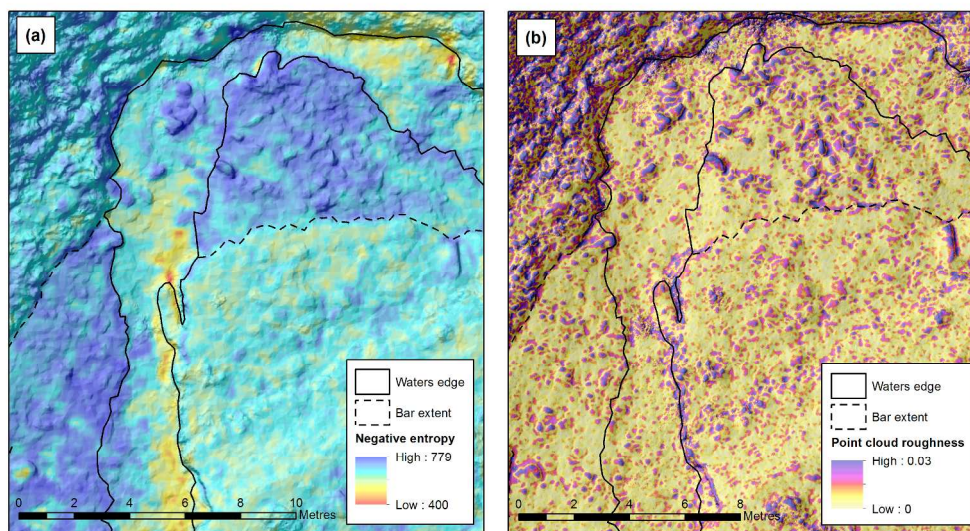


Figure 2. Examples outputs of (a) negative image entropy and (b) point cloud roughness for a subsection of the Coledale Beck site.

289x161mm (300 x 300 DPI)

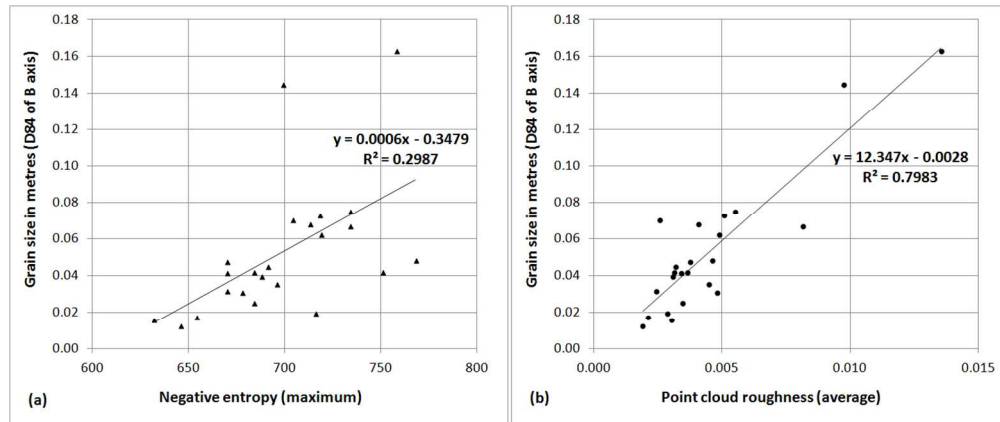


Figure 3. Calibration relationships between (a) negative image entropy (texture) and (b) point cloud roughness, with grain size.

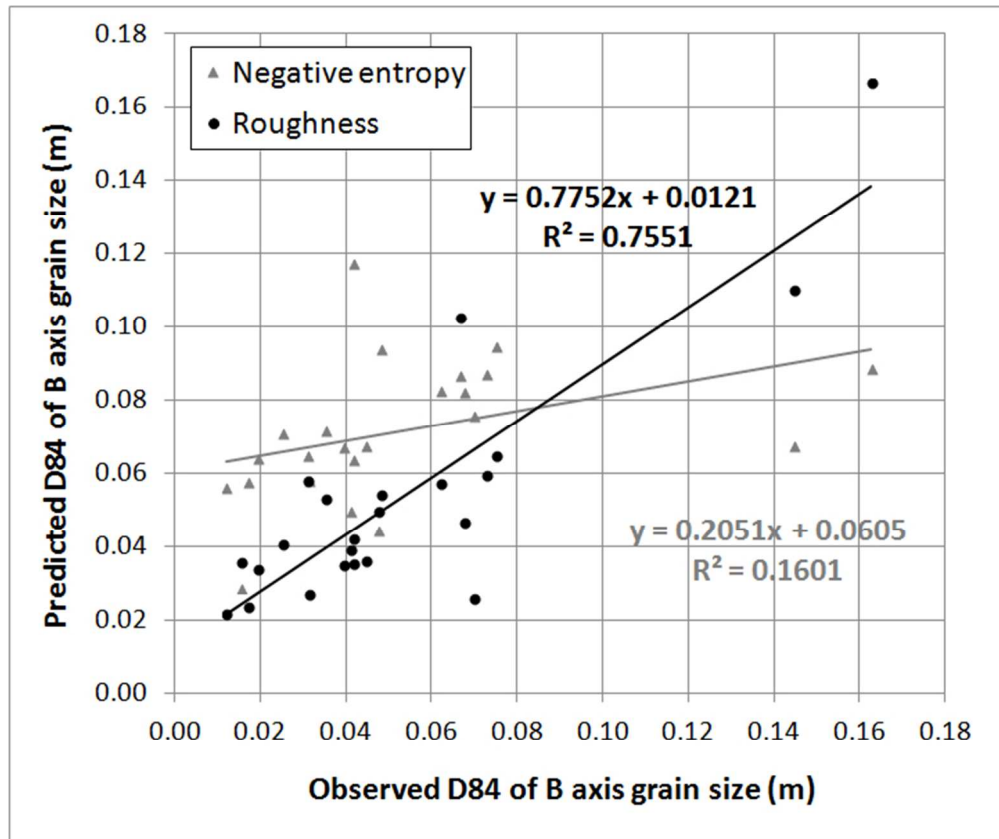


Figure 4. Grain size predicted from negative image entropy and point cloud roughness methods, versus observed grain size (D84 of B axes). N = 23, p < 0.01 for both regressions.

view